SJMI(2018) 01;29-37 ISSN : 2635-4608

DOI http://dx.doi.org/10.31916/sjmi2018-01-3

T2-weighted MRI of breast cancer using hyaluronic acid coated magnetic nanoparticles as a tool of contrast agent

Sangbock Le [a,b+], *Hwayeon Yeo* [b], *Byungju Ahn* [b], *V. R. Singh* [c], *Nguyen Van Do* [d]

Received: 25 May 2018 / Accepted: 22 July 2018 / Published online: 1 September 2018

ABSTRACT Novel diagnostic technique has been developed in many research area using targetable contrast agents with magnetic resonance imaging (MRI) for cancer diagnosis. It is efficient for cancer diagnosis to use MRI with biocompatible targeting moiety and magnetic nanoparticles (MNPs). Thus, we synthesized MNPs using thermal decomposition method which enable sensitive T2- or T2 Turbo spin echo (TSE) weighted magnetic resonance imaging. And it was coated with Hyaluronic acid (HA). Also we carried out that breast cancer cell line (MDA-MB-231) which has cancer stem cell property was injected in heterotopic mouse model. And then magnetic resonance sequence (T2) for imaging effects and targeting ability were analyzed into MNPs conjugated HA. We noted that MDA-MB-231 cell which high-expressed CD44 ligand was showed contrast enhance efficiency through magnetic nanoparticles because of combining a lot of HA As a result of these studies, we conclude that HA coated magnetic nanoparticles can be effectively used as a novel probe for visualizing of Breast cancer stem cell.

Key words: contrast agent, gastric cancer, CD44, magnetic nanoparticles, magnetic resonance imaging

Keywords : T2-weighted MRI, Hyaluronic acid coating, Magnetic Nano Particles, Contrast Agents

[a,b+]S. B. Lee ✉
Correspondence to: Sangbock Lee
Dept. of Radiology, Nambu University

[b]Hwayeon Yeo
Dept. of Radiology, Nambu University
e-mail : yhy@gmail.com

[b]Byungju Ahn
Dept. of Radiology, Nambu University
e-mail : anju6010@gmail.com

[c]V. R. Singh
Director, PDM University, India
e-mail : vr-singh@ieee.org

[d]Nguyen Van Do
Dept. of Nuclear Engineering, Hanoi University of Science and Technology
e-mail : vr-nguyen.van.do@hust.edu.vn

1. Introduction

Molecular imaging provides as a tool to diagnose cancer at the cellular and molecular levels. It not only allows early and accurate tumor localization in diagnostic cancer imaging, but also has a potential to visualize the biological processes of tumor growth, metastasis and response to treatment.(1-10) Molecular MR imaging (Magnetic resonance imaging) has emerged as a key factor for the diagnosis of cancer.(11-18) Since it has advantages over noninvasive, good anatomical image due to high resolution,

high contrast and 3-dimensional information in real time more than nuclear medicine (PET, SPECT), optical imaging compared to other imaging modality.(19-23) And also, molecular MR imaging is able to detect simultaneously metabolism of cells and tissues and its physiological information and structural information, noninvasive and biological processes occurring in the deep tissues to provide the quantitative information.(24,25) Molecular MR imaging can observe a variety of imaging lesions as multi-modality in the diagnosis of breast cancer.

Many MR contrast agents have been used for good quality imaging (32-37). However passive contrast agents are not enough to reach their target goals specifically. Thus, we are aiming to develop intelligent targetable contrast agent using Hyaluronic acid (HA)(38-44). In particular, HA has become known to interact on CD44 receptor. Then breast cancer is known to being overexpressed CD44 receptor which as marker of cancer stem cell.(44) It is so crucial for MR probe to early breast cancer diagnostic point of view. Because CD44, important as cancer stem cell marker, is interacted with Hyaluronic acid. Hyaluronic acid which is a linear hydrogel with negative charge containing two alternating units of D-glucuronic acid (GLcUA) and N-acetyl-D-glucosamine (GLcNAc) with molecular weight of 105–107. HA has frequently been used for medical purposes such as a viscoelastic biomaterial in surgery. Especially, it is well known that various human tumor cells (breast, ovarian, colon, lung, stomach, etc.) over-express HA-binding receptors, CD44 (44) In this study, molecular MR imaging were investigated to find biological processes which occur in gastric cancer. T2 weight sequence was simultaneously used to confirm for better diagnostic possibility and targeting effect was demonstrated through Hyaluronic acid conjugated magnetic nanoparticles in heterotopic xenograft breast cancer model. And various experiments were conduct to evaluate specific binding affinity and diagnostic effectiveness through in vivo and in vitro.

2. RESULT AND DISCUSSION

2.1 Preparation of MNPs and HA-MNPs

Monodispersed magnetic nanoparticles were synthesized using thermal decomposition and solubilized in nonpolar organic solvent, as previously reported. And HA conjugated MNP was synthesized using EDC and sulfo-NHS method. As shown in (Fig. 1), the characteristic band of HA-MNPs conjugates were verified by FT-IR spectra, which exhibits O-H stretching at 3200-3400cm^{-1} , C=O stretching at 1100-1300cm^{-1} , CO-NH(amide) bonds at 1630-1680cm^{-1} and CH_2 bending in HA at 1430-1470cm^{-1} .

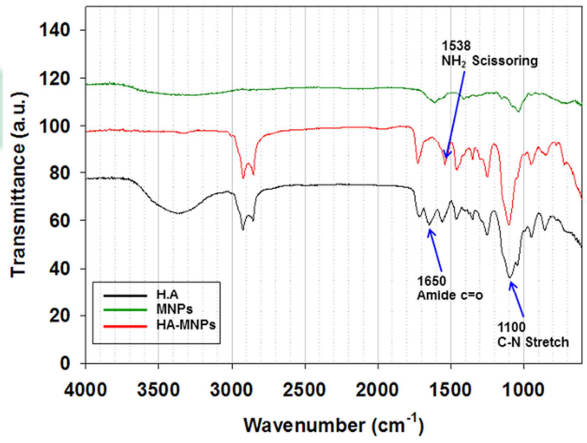

Fig.1. Fourier transform infrared spectra of HA (green line), MNP (red line) and HA-MNP(black line), i:CO-NH(amide) bonds

As MR agents, uniform MNPs (12nm) were synthesized at a high temperature via a thermal decomposition process. The size distribution and morphology of MNPs were confirmed by transmission electron microscopy (Fig. 2.) which showed no significant differences in size or morphology between HA-MNPs and MNP. The size of the

water-soluble MNPs and HA-MNPs were determined to be 84.6 ± 32.4nm and 137 ± 53.2nm, respectively. After the conjugation of Hyaluronic acid MNPs, the size slightly increased due to the large molecular weight of Hyaluronic acid (1000kDa). In addition, the surface charge of aminated MNPs also changed from 20.62 ± 1.96 mV(aminated water soluble MNP) to -17.76 ± 1.64 mV (HA coated MNP) due to the presence of HA (Fig. 2.).

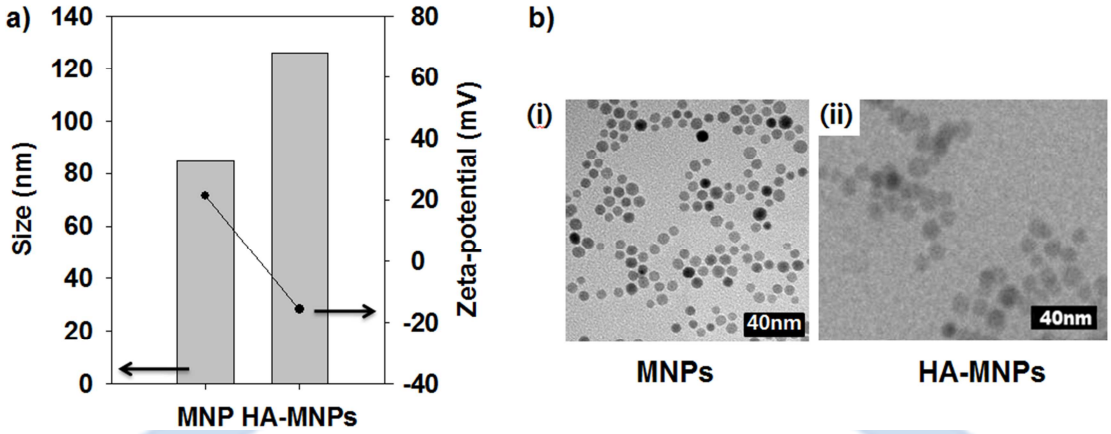

Fig.2. . (a) is The average size (gray bar) and zeta potential (black circle) and (b) is TEM images of (i) magnetic nanoparticles (ii) hyaluronan-modified magnetic nanoparticles (HA-MNP)

2.2 Solubility and magnetic sensitivity of HA-MNPs

To assess the potential use of HA-MNPs as MR imaging agents, we performed MR imaging experiments using HA-MNPs, exhibiting the highest magnetic properties with appropriate size to avoid RES detection and prolong retention in the circulation. In Fig. 2 (a) (i), the T2-weighted MR image exhibited a strong black color, which signified a decrease in signal intensity for the thicker HA-MNP solution. In Fig. 2 (b) (ii) represent change of intensity between of T2-weighted MR solution image

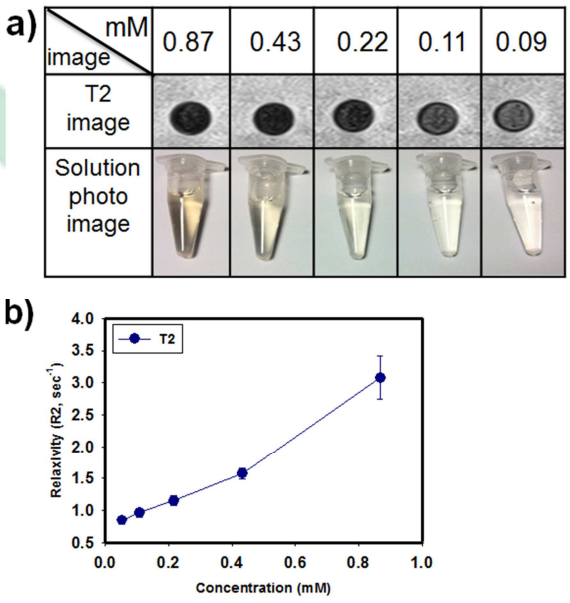

Fig.3. (a) Photographs and T2 solution MR images of HA-MNPs each conditions and (b) R2 relaxivity graph for the

magnetic ion concentration.

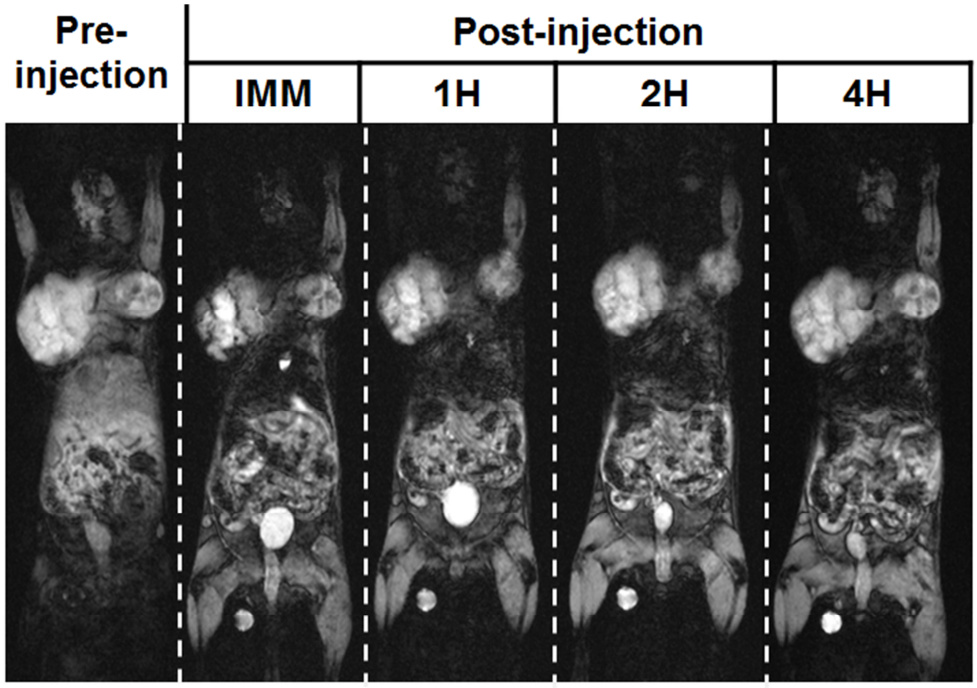

Fig.4. T2 MR images of tumor-bearing mice after intravenous injection of HA-MNPs. FOV: 100mm, ST: 1.00mm, TR: 14.85ms, TE: 5.65ms, coil elements: Wrist coil, Imaging modality: Siemens MR scanner

2.4 In vivo MR image

In Fig. 4, MR signal enhancement was identified after HA-MNPs injection. Initially, the center of tumor instantly darkened, and enhanced MR imaging signal intensity at surrounding vessels was simultaneously observed. In T2 weight MR images, clear anatomic details were observed,

3. CONCLUSION

In summary, we synthesized HA-MNPs as MR imaging agents for effective diagnosis for CD44-overexpressing breast cancer.. Further study, we plan to evaluate as a molecular imaging tool using variable MR sequence for better imaging technique.

4. EXPERIMENTAL METHOD

4.1. Materials

Polysorbate 80, ethylenediamine, 1,4-dioxane (99.8%), 4-dimethylaminopyridine, triethylamine, and succinic anhydride (SA) were purchased from Sigma Aldrich Chemical Co. Phosphate buffered saline (PBS: 10 mM, pH 7.4), Roswell Park Memorial Institute-1640 (RPMI-1640), fetal bovine serum and antibiotic-antimycotic solution were purchased from Gibco and dialysis membrane (molecular weight cut off: 1,000 Da) was obtained from Spectrum laboratory. Hyaluronic acid (HA, 1,000,000 Da) was purchased from Yuhan Phrmaceutical Corporation (Seoul, Korea). MDA-MB-231 cell lines (American Type Culture Collection) were grown in medium containing 10% fetal bovine serum and 1% Antibiotic-Antimycotic at 37℃, humidified 5% CO_2 atmosphere.

4.2. Synthesis of magnetic nanoparticles

To synthesize monodispersed magnetic nanoparticles (MNPs), 2 mmol of iron (III) acetylacetonate, 1 mmol of manganese(II) acetylacetonate, 10 mmol of 1,2-hexadecanediol, 6 mmol of dodecanoic acid, and 6 mmol of dodecylamine were dissolved in 20 mL of benzyl ether under an ambient nitrogen atmosphere. The mixture was then pre-heated to 200°C for 2 hours and refluxed at 300°C for 30 minutes. After the reactants were cooled at room temperature, the products were purified with an excess of pure ethanol. Approximately 11 nm of MNPs were synthesized using the seed-mediated growth method.

4.3. Preparation of hyaluronan-modified magnetic nanoparticles (HA-MNPs)

HA-MNPs were prepared by the nano-emulsion method. 30 mg of magnetic nanoparticle were dissolved in 4 mL hexane (organic phase). This organic phase was poured into 20 mL deionized water (aqueous phase) containing 30 mg HA. The solution was ultra-sonicated in an ice-cooled bath for 20 min at 190W and stirred overnight at room temperature to evaporate the organic solvent. The resulting suspension was centrifuged three times for 20 min each at 3000 rpm. After the supernatant was removed, the precipitated HA-MNPs were re-dispersed in 5 Ml deionized water. The size distribution and zeta potential of HA-MNPs were analyzed by laser scattering (ELS-Z, Otsuka Electronics); morphologies were confirmed using a transmittance electron microscope (TEM, JEM-2100, JEOL Ltd. Japan.). Finally, the relaxivity (R2) data of HA-MNPs solution were measured through magnetic resonance (MR) imaging analysis.

4.7. Heterotopic animal model and experimental procedure

All animal experiments were conducted with the approval of the Association for Assessment and Accreditation of Laboratory Animal Care (AAALAC) International. Female BALB/C-Slc nude mice at 7-8 weeks of age were anesthetized by intraperitoneal injection of a Zoletil/Rompun mixture and injected with 200 mL containing. 1.0 x 10^7 MDA-MB-231 cells suspended in saline into the femoral region. After cancer cell implantation, MR imaging was performed between 2 and 3 weeks. After MR imaging organ MR imaging performed too. In addition, the extracted tumor tissues from tumor-bearing mice treated with HA-MNPs were frozen, sectioned, and stained using Prussian blue. All stained tissue sections were analyzed using a virtual microscope (Olympus BX51, Japan) and Olyvia software.

4.8. MR imaging

Animal, organ, solution and cell MR imaging experiments were performed with a 3 Tesla Siemens clinical MRI instrument using a wrist coil with T2 Turbo spin echo sequence. (T2 Turbo spin echo: TR: 4000ms, TE : 114ms ,Slice thickness : 1.0mm, FOV read : 180mm)

Acknowledgments

This study was supported by research funds from Nambu University, 2017.

Reference

[1] Kim JK, Choi KJ, Lee M, Jo MH, Kim S. Molecular imaging of a cancer-targeting theragnostics probe using a nucleolin aptamer- and microRNA-221 molecular beacon-conjugated nanoparticle. Biomaterials 2012;33(1):207-217.

[2] Kircher MF, Hricak H, Larson SM. Molecular imaging for personalized cancer care. Molecular oncology 2012;6(2):182-195.

[3] Meng X, Loo BW, Jr., Ma L, Murphy JD, Sun X, Yu J. Molecular imaging with 11C-PD153035 PET/CT predicts survival in non-

small cell lung cancer treated with EGFR-TKI: a pilot study. Journal of nuclear medicine : official publication, Society of Nuclear Medicine 2011;52(10):1573-1579.

[4] Gong P, Shi B, Zheng M, Wang B, Zhang P, Hu D, Gao D, Sheng Z, Zheng C, Ma Y, Cai L. PEI protected aptamer molecular probes for contrast-enhanced in vivo cancer imaging. Biomaterials 2012.

[5] Blasberg RG. Molecular imaging and cancer. Molecular cancer therapeutics 2003;2(3):335-343.

[6] Hoffman JM, Menkens AE. Molecular imaging in cancer: future directions and goals of the National Cancer Institute. Academic radiology 2000;7(10):905-907.

[7] Bzyl J, Lederle W, Rix A, Grouls C, Tardy I, Pochon S, Siepmann M, Penzkofer T, Schneider M, Kiessling F, Palmowski M. Molecular and functional ultrasound imaging in differently aggressive breast cancer xenografts using two novel ultrasound contrast agents (BR55 and BR38). European radiology 2011;21(9):1988-1995.

[8] Nishino M, Jackman DM, Hatabu H, Janne PA, Johnson BE, Van den Abbeele AD. Imaging of lung cancer in the era of molecular medicine. Academic radiology 2011;18(4):424-436.

[9] Kiessling F. Science to practice: the dawn of molecular US imaging for clinical cancer imaging. Radiology 2010;256(2):331-333.

[10] Pinker K, Stadlbauer A, Bogner W, Gruber S, Helbich TH. Molecular imaging of cancer: MR spectroscopy and beyond. European journal of radiology 2012;81(3):566-577.

[11] Artemov D, Mori N, Okollie B, Bhujwalla ZM. MR molecular imaging of the Her-2/neu receptor in breast cancer cells using targeted iron oxide nanoparticles. Magnetic resonance in medicine : official journal of the Society of Magnetic Resonance in Medicine / Society of Magnetic Resonance in Medicine 2003;49(3):403-408.

[12] Gossmann A, Okuhata Y, Shames DM, Helbich TH, Roberts TP, Wendland MF, Huber S, Brasch RC. Prostate cancer tumor grade differentiation with dynamic contrast-enhanced MR imaging in the rat: comparison of macromolecular and small-molecular contrast media--preliminary experience. Radiology 1999;213(1):265-272.

[13] Tan MQ, Burden-Gulley SM, Li W, Wu XM, Lindner D, Brady-Kalnay SM, Gulani V, Lu ZR. MR Molecular Imaging of Prostate Cancer with a Peptide-Targeted Contrast Agent in a Mouse Orthotopic Prostate Cancer Model. Pharmaceutical research 2012;29(4):953-960.

[14] Pinker K, Stadlbauer A, Bogner W, Gruber S, Helbich TH. Molecular imaging of cancer: MR spectroscopy and beyond. European journal of radiology 2012;81(3):566-577.

[15] Song HT, Suh JS. Cancer - Targeted MR Molecular Imaging. J Korean Med Assoc 2009;52(2):121-124.

[16] Grenier N, Quesson B, de Senneville BD, Trillaud H, Couillaud F, Moonen C. Molecular Mr Imaging and Mr-Guided Ultrasound Therapies in Cancer. JBR-BTR

2009;92(1):8-12.

[17] Artemov D, Mori N, Okollie B, Bhujwalla ZM. MR molecular imaging of the Her-2/neu receptor in breast cancer cells using targeted iron oxide nanoparticles. Magnet Reson Med 2003;49(3):403-408.

[18] Gossmann A, Okuhata Y, Shames DM, Helbich TH, Roberts TPL, Wendland MF, Huber S, Brasch RC. Prostate cancer tumor grade differentiation with dynamic contrast-enhanced MR imaging in the rat: Comparison of macromolecular and small-molecular contrast media - Preliminary experience. Radiology 1999;213(1):265-272.

[19] Thomas D, Bal H, Arkles J, Horowitz J, Araujo L, Acton PD, Ferrari VA. Noninvasive assessment of myocardial viability in a small animal model: comparison of MRI, SPECT, and PET. Magnetic resonance in medicine : official journal of the Society of Magnetic Resonance in Medicine / Society of Magnetic Resonance in Medicine 2008;59(2):252-259.

[20] Coimbra A, Williams DS, Hostetler ED. The role of MRI and PET/SPECT in Alzheimer's disease. Current topics in medicinal chemistry 2006;6(6):629-647.

[21] Spencer SS, Theodore WH, Berkovic SF. Clinical applications: MRI, SPECT, and PET. Magnetic resonance imaging 1995;13(8):1119-1124.

[22] Kim AY, Han JK, Seong CK, Kim TK, Choi BI. MRI in staging advanced gastric cancer: is it useful compared with spiral CT? Journal of computer assisted tomography 2000;24(3):389-394.

[23] Portnoi LM, Denisova LB, Stashuk GA, Nefedova VO. [Magnetic resonance imaging in the diagnosis of gastric cancer: X-ray versus MRI anatomic findings]. Vestnik rentgenologii i radiologii 2000(1):26-40.

[24] Bradbury M, Hricak H. Molecular MR imaging in oncology. Magnetic resonance imaging clinics of North America 2005;13(2):225-240.

[25] Delikatny EJ, Poptani H. MR techniques for in vivo molecular and cellular imaging. Radiologic clinics of North America 2005;43(1):205-220.

[26] de Zwart IM, de Roos A. MRI for the evaluation of gastric physiology. European radiology 2010;20(11):2609-2616.

[27] Takeda M, Amano Y, Machida T, Kato S, Naito Z, Kumita S. CT, MRI, and PET findings of gastric schwannoma. Japanese journal of radiology 2012.

[28] Motohara T, Semelka RC. MRI in staging of gastric cancer. Abdominal imaging 2002;27(4):376-383.

[29] Spieth ME, Gauger BS. Time-resolved 3D MRI of gastric emptying. AJR American journal of roentgenology 2004;182(1):259; author reply 259.

[30] Das CJ, Debnath J, Mukhopadhyay S. MRI appearance of giant gastric lymphangioma. Indian journal of gastroenterology : official journal of the Indian Society of Gastroenterology 2006;25(2):81.

[31] Kim IY, Kim SW, Shin HC, Lee MS, Jeong DJ, Kim CJ, Kim YT. MRI of gastric carcinoma: results of T and N-staging in an in vitro study. World journal of gastroenterology : WJG 2009;15(32):3992-3998.

[32] Tan M, Burden-Gulley SM, Li W, Wu X, Lindner D, Brady-Kalnay SM, Gulani V, Lu ZR. MR molecular imaging of prostate cancer with a peptide-targeted contrast agent in a mouse orthotopic prostate cancer model. Pharmaceutical research 2012;29(4):953-960.

[33] Buijs M, Kamel IR, Vossen JA, Georgiades CS, Hong K, Geschwind JF. Assessment of metastatic breast cancer response to chemoembolization with contrast agent enhanced and diffusion-weighted MR imaging. Journal of vascular and interventional radiology : JVIR 2007;18(8):957-963.

[34] Rydland J, BjOrnerud A, Haugen O, Torheim G, Torres C, Kvistad KA, Haraldseth O. New intravascular contrast agent applied to dynamic contrast enhanced MR imaging of human breast cancer. Acta Radiol 2003;44(3):275-283.

[35] Nikolaou K, Kramer H, Grosse C, Clevert D, Dietrich O, Hartmann M, Chamberlin P, Assmann S, Reiser MF, Schoenberg SO. High-spatial-resolution multistation MR angiography with parallel imaging and blood pool contrast agent: initial experience. Radiology 2006;241(3):861-872.

[36] Stracke CP, Katoh M, Wiethoff AJ, Parsons EC, Spangenberg P, Spuntrup E. Molecular MRI of cerebral venous sinus thrombosis using a new fibrin-specific MR contrast agent. Stroke; a journal of cerebral circulation 2007;38(5):1476-1481.

[37] McDannold N, Fossheim SL, Rasmussen H, Martin H, Vykhodtseva N, Hynynen K. Heat-activated liposomal MR contrast agent: initial in vivo results in rabbit liver and kidney. Radiology 2004;230(3):743-752.

[38] Lim EK, Kim HO, Jang E, Park J, Lee K, Suh JS, Huh YM, Haam S. Hyaluronan-modified magnetic nanoclusters for detection of CD44-overexpressing breast cancer by MR imaging. Biomaterials 2011;32(31):7941-7950.

[39] He Y, Wu GD, Sadahiro T, Noh SI, Wang H, Talavera D, Vierling JM, Klein AS. Interaction of CD44 and hyaluronic acid enhances biliary epithelial proliferation in cholestatic livers. American journal of physiology Gastrointestinal and liver physiology 2008;295(2):G305-312.

[40] Knupfer MM, Poppenborg H, Hotfilder M, Kuhnel K, Wolff JE, Domula M. CD44 expression and hyaluronic acid binding of malignant glioma cells. Clinical & experimental metastasis 1999;17(1):71-76.

[41] Miyake H, Hara I, Okamoto I, Gohji K, Yamanaka K, Arakawa S, Saya H, Kamidono S. Interaction between CD44 and hyaluronic acid regulates human prostate cancer development. The Journal of urology 1998;160(4):1562-1566.

[42] Lesley J, Hyman R. CD44 can be activated to function as an hyaluronic acid receptor in normal murine T cells. European journal of immunology 1992;22(10):2719-2723.

[43] Hyman R, Lesley J, Schulte R. Somatic cell

mutants distinguish CD44 expression and hyaluronic acid binding. Immunogenetics 1991;33(5-6):392-395.

[44] Zhang W, Gao L, Qi S, Liu D, Xu D, Peng J, Daloze P, Chen H, Buelow R. Blocking of CD44-hyaluronic acid interaction prolongs rat allograft survival. Transplantation 2000;69(4):665-667.